# Near-IR Cavity Ringdown Spectroscopy and Kinetics of the Isomers and Conformers of the Butyl Peroxy Radical

**Brent G. Glover and Terry A. Miller***

*Laser Spectroscopy Facility, Department of Chemistry, The Ohio State University, 120 West 18th Avenue, Columbus, Ohio 43210*

*Received: August 26, 2005; In Final Form: October 13, 2005*

Cavity ringdown spectra of butyl peroxy radicals have been obtained for their $\tilde{A}-\tilde{X}$ electronic transition in the near-IR. The radicals were produced by two independent chemical methods, allowing unambiguous assignment of the spectra of the four butyl peroxy isomers with probable conformer assignments also possible for a number of cases. Using the analyzed spectra semiquantatively, isomer specific rate constants for butyl peroxy self-reaction were measured, as was the relative reactivity of the various sorts of H atoms in butane to Cl atom attack.

## 1. Introduction

Some of the most important reactive intermediates[1] in low-temperature combustion and other processes involving the oxidation of organic molecules are the peroxy radicals ($RO_2$). In combustion, the competition between hydrocarbon radical reaction with $O_2$ to form peroxy radicals and hydrocarbon radical self-reaction is critical to the amount of soot produced.[2] In the troposphere, any volatile organic compound (RH) present is oxidized[3] primarily by an initial reaction with OH to produce a R radical that subsequently combines with $O_2$ in a three-body process to form a peroxy radical, $RO_2$. In clean atmospheres, organic peroxy radicals undergo self-reaction, cross-reactions, or reaction with $HO_2$ to generate alcohols, carbonyl compounds, and hydroperoxides, which are subsequently involved in a variety of important atmospheric processes. In polluted atmospheres, the reaction of $RO_2$ with NO produces $NO_2$, which is subsequently photolyzed to produce oxygen atoms that react with $O_2$ to produce $O_3$. It has been estimated that the reactions of peroxy radicals are responsible for ≈90% of the ozone present in the troposphere.[3]

Historically, peroxy radical reactions have been monitored[4] by their $\tilde{B}-\tilde{X}$ electronic absorption spectrum in the UV. However, the $\tilde{B}$ state is dissociative, leading to a broad, structureless $\tilde{B}-\tilde{X}$ absorption, whose appearance is only weakly dependent on the R group of the organic peroxy. Though a relatively sensitive means of $RO_2$ detection, the $\tilde{B}-\tilde{X}$ absorption has poor selectivity among the various $RO_2$ radicals.

We have pioneered efforts to use cavity ringdown spectroscopy (CRDS) to sensitively detect $RO_2$ radicals via their $\tilde{A}-\tilde{X}$ electronic transition in the near-infrared (NIR). Because this is a bound−bound transition with well-defined structure, NIR CRDS is capable of distinguishing not only among different chemical species $RO_2$ and $R'O_2$ but also among different isomers, and even conformers, of a given $RO_2$ radical. For the peroxy radicals, where R is a simple alkyl group, we have reported NIR CRDS with R = $CH_3$,[5] $C_2H_5$,[5] and 1- and 2-$C_3H_7$.[6,7]

Larger alkanes play significant roles in both combustion and atmospheric chemistry. It is therefore worthwhile examining the $\tilde{A}-\tilde{X}$ spectra of the corresponding $RO_2$ radicals. In this report, we turn our attention to the case of R = $C_4H_9$. There are four distinct butyl peroxy isomers: two formed from primary substitution, *n*-butyl peroxy and isobutyl peroxy; one formed by secondary substitution, *sec*-butyl; and one formed from tertiary substitution, *tert*-butyl peroxy. These isomers are presented pictorially in Figure 1.

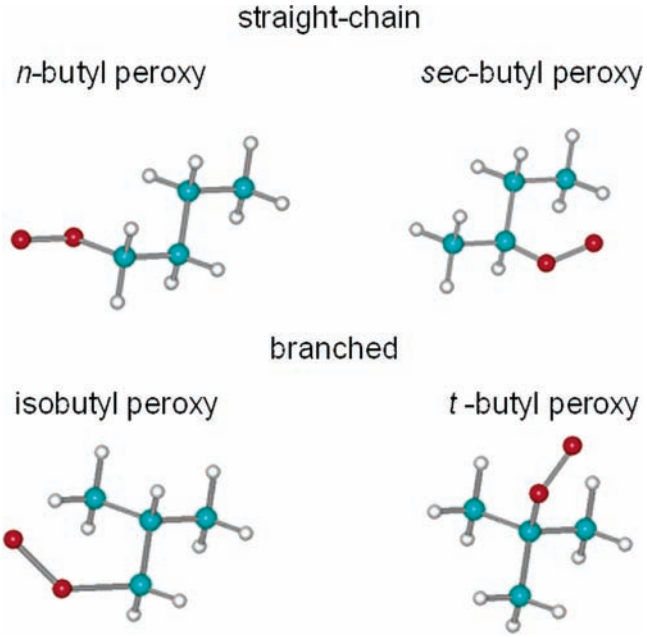


**Figure 1.** Four isomers of butyl peroxy radical, $C_4H_9O_2$.

In the following, we describe the NIR CRDS spectra of all of the butyl peroxy isomers. We also distinguish among the spectra of different conformers of a given isomer. Using these spectra as highly specific diagnostics of a given species, we are able to make some preliminary observations about the butyl peroxy radicals' surprisingly diverse reaction kinetics.

## 2. Experimental Section

**2.1. NIR CRDS Apparatus.** The apparatus was similar to that used in previous studies of the $\tilde{A}-\tilde{X}$ spectroscopy of the alkyl peroxy radicals.[5,6,8] Briefly, the second harmonic light from an Nd:YAG laser pumped a dye laser (20 Hz Quanta-Ray PRO-

10.1021/jp054838q CCC: $30.25 © 2005 American Chemical Society
Published on Web 11/17/2005

270 Nd:YAG, Spectra Physics SIRAH dye laser). The dyes used were DCM, Rhodamine B, and Rhodamine 101. The dye laser was tuned over the 660−585 nm region with pulse energies of 80−100 mJ and a laser line width of 0.03 $cm^{-1}$ (fwhm). The near-IR light required for the ringdown cell was produced by Raman shifting the dye laser light using molecular hydrogen. A 50 cm focal length lens focused the laser beam through the middle of a 70 cm long single-pass Raman cell pressurized with 200−300 psi of molecular hydrogen. The useful second Stokes radiation was generated in the region of 1460−1140 nm (6850−8770 $cm^{-1}$), whereas the unused first Stokes, fundamental, and anti-Stokes radiation was filtered out using several 1000 nm long-pass cutoff filters. Before the 1−2 mJ of NIR light entered the ringdown cell, it passed through two lenses, each with 1 m focal length, to approximate a $TEM_{00}$ cavity mode.[9]

A highly reflective ($R \geq 99.99\%$) plano-concave mirror (Los Gatos Research) with a 6 m curvature was placed at each end of the 55 cm long ringdown cell. Mirrors were attached to the stainless steel cell using fine adjustment mounts. Because the desired wavelength range of the NIR light was 1460−1140 nm, three sets of mirrors were used to cover this range. Each mirror set had sufficient overlap to allow complete wavelength coverage. To protect the mirrors from any harsh chemicals present in the cell, a constant flow of nitrogen purged the exposed surface of the mirrors. Along with purge inlets, the ringdown cell was constructed with inlets for precursor gases, a Baratron pressure gauge, and an exhaust leading to a mechanical pump. UV grade quartz windows covered the two rectangular apertures (2 cm × 18 cm) on either side of the ringdown cell. The inner width of the ringdown cell between the two windows was 2.3 cm.

The NIR radiation that passed through both highly reflective mirrors and exited the ringdown cell was focused by a 2.5 cm focal length lens onto an amplified InGaAs photodiode. The signal from the photodiode detector was digitized by a 12 bit 20 MHz digitizing card installed in the PC controlling the experiment. For CRDS spectra, the signals of twenty consecutive laser shots were averaged at each dye laser frequency point. Using the nonlinear Levenberg−Marquardt algorithm, the digitized signal of observed decay of radiation was fit to a single exponential to acquire ringdown time, initial amplitude, and baseline. The ringdown time was converted to the cavity absorption per pass (ppm) and saved as a point in the spectrum. At each frequency point, a ringdown time was acquired with the photolysis excimer laser on and off. Taking the difference between the two traces removed the background structures, i.e., broad bands of precursor absorption and the sharp rotationally resolved water lines, yielding spectra of molecules produced as a result of photolysis.

To initiate the chemistry producing $C_4H_9O_2$ radicals, the radiation from the photolysis excimer laser (LPX300, Lambda Physik) operating at 193 nm was focused by a cylindrical and a spherical lens to a rectangular shape of 0.5 cm × 13 cm. Fifty microseconds before each shot of NIR light entered the cavity, the excimer radiation passed once through the ringdown cell by way of the UV-grade quartz windows. The flux of excimer radiation passing through the ringdown cell was $\approx 7 \times 10^{15}$ photons/$cm^2$.

**2.2. Production of Butyl Peroxy Radicals.** Two methods of peroxy radical production were used. Initially, butyl radicals were produced by either direct photolysis of butyl bromides or hydrogen abstraction of butane via photolysis of oxalyl chloride to produce Cl atoms. The butyl radicals subsequently reacted with $O_2$ to produce peroxy via a 3-body collision involving $N_2$.

*2.2.1. Direct Photolysis of Butyl Bromides.* The precursor molecules used in the direct photolysis method were brominated butanes. The bromides were chosen because the carbon−bromine bond will easily break during 193 nm photolysis.[10] The photolytic production of butyl radical from $C_4H_9Br$ took place in the presence of oxygen and nitrogen, the latter acting as a third body that was capable of removing excess energy from the excited butyl peroxy radical formed from the reaction of the $C_4H_9$ radical and $O_2$. A given isomer of butyl peroxy radical was produced by photolyzing the corresponding isomer of butyl bromide, yielding isomer-specific CRDS spectra.

Nitrogen was passed into a vessel containing butyl bromide, bubbling through the liquid before exiting the container, mixing with oxygen, and entering the ringdown cell. Typical concentrations (in Torr) of reactants used for the direct photolysis method of peroxy radical production included $[C_4H_9Br] \sim 5$, $[O_2] = 100$, $[N_2] = 50$. Assuming unity quantum yield for butyl radical and an absorption cross section[11] for butyl bromide of $5 \times 10^{-19}$ $cm^2$/molecule with the estimated $7 \times 10^{15}$ $cm^{-2}$ flux of 193 nm photons, the number of $C_4H_9$ radials produced can readily be calculated to be $\approx 6 \times 10^{14}$ $cm^{-3}$.

The advantage of the direct photolysis method is that one isomer of butyl peroxy radical is produced for a given precursor. The disadvantage comes from the broad precursor absorption in the NIR region. This background can be subtracted along with other background features, such as water lines. Nevertheless, the precursor absorption increases the baseline of the spectra from 100 to 1000 ppm. In addition, as is shown below, the net production of radical per photolysis photon is not as great as with the alternative H-atom abstraction technique described below. Therefore, though the CRDS spectra acquired with the direct photolysis of butyl bromides are isomer specific, the signal-to-noise ratio is not advantageous.

*2.2.2. Hydrogen Abstraction via Photolysis of Oxalyl Chloride.* The alternative method of peroxy radical production was photolysis of oxalyl chloride, $(COCl)_2$, to produce chlorine atoms for hydrogen abstraction from the butane molecule. The probable butyl peroxy radical production mechanism is

$$(COCl)_2 \xrightarrow{193\ nm} 2Cl + 2CO \quad (1)$$

$$C_4H_{10} + Cl \rightarrow C_4H_9 + HCl \quad (2)$$

$$C_4H_9 + O_2 + N_2 \rightarrow C_4H_9O_2 + N_2 \quad (3)$$

Oxalyl chloride has a large absorption cross section $\sigma_{OxCl} = 3.8 \times 10^{-18}$ $cm^2$ at 193 nm, and only chlorine atoms and carbon monoxide have been reported[12,13] as dissociation products. For production of *n*-butyl and *sec*-butyl peroxy radical, *n*-butane was used. For production of isobutyl and *tert*-butyl peroxy radical, isobutane was the precursor. Typical concentrations (in Torr) of reactants used for the hydrogen abstraction method of peroxy radical production included $[(COCl)_2] = 0.5$, $[C_4H_{10}] = 2$, $[O_2] = 80$, $[N_2] = 150$. Using the same photolysis flux of 193 nm photons as before, and assuming a yield of two chlorine atoms per photon absorbed, result in a total production of $9 \times 10^{14}$ $cm^{-3}$ of the two isomers of $C_4H_9$ radicals.

The hydrogen abstraction method of peroxy radical production produces more radicals than the direct photolysis method and also has less background in the NIR. Although more than one isomer is produced at a time, the hydrogen abstraction method results in CRDS spectra with significantly greater signal-to-noise ratio.

### 3. Structural Overview of Butyl Peroxy Radicals

It is worthwhile reviewing briefly what is known from quantum chemistry calculations and experiment about the simpler alkyl peroxy radicals with R = $CH_3$, $C_2H_5$, and $C_3H_7$. Obviously, methyl peroxy, $CH_3O_2$, is the simplest species and only a single isomeric form with a peroxy-like electronic structure, and hence chemical reactivity, is possible. One can envision two possible distinct conformers. One is a cis form when the $O_2$ group is staggered with respect to the methyl H's. There could also be a trans conformation with the terminal O and a methyl H eclipsed. However, this trans conformation is found by calculation[5,14,15] to be a saddle point representing a barrier to methyl group (or equivalently $O_2$) rotation. Correspondingly, only one conformation has ever been observed spectroscopically and it has (somewhat resolved) rotational structure consistent with the cis conformation.

Moving to ethyl peroxy, $C_2H_5O_2$, it again is clear that only one peroxy-like isomer is possible. However, now calculations indicate two stable conformers,[16,17] T (trans) and G (gauche) versions corresponding to 0° and 120° (−120°) for the dihedral angle between the O−O−C and O−C−C planes. Although the calculation indicates an energy separation between the T and G forms of $<kT$ at room temperature, the spectrum of only one conformer has been reported experimentally.[5] However, the observed spectrum does contain some unassigned structure.

Moving to propyl peroxy, $C_3H_7O_2$, the situation becomes more complex. There are two peroxy-like isomeric forms, 1-propyl (or *n*-propyl) and 2-propyl (or isopropyl) peroxy. From computations,[7,18] the latter has two stable conformers T (with $C_s$ symmetry) and G, which correspond to the C−O−O plane coinciding with the plane bisecting the C−C−C angle and lying at 120°, respectively. 1-Propyl peroxy has five stable conformers with $T_1(G_1)$ specifying the dihedral angle between the O−O−C and O−C−C planes and $T_2(G_2)$ the angle between the O−C−C and C−C−C planes. The resulting conformers are $T_1T_2$, $T_1G_2$, $G_1T_2$, $G_1G_2$, and $G_1'G_2$ with G denoting a +120° rotation and G′ a −120° rotation from the T conformation. (For each conformer with a G form there is a correspondingly G′ mirror image that is not spectroscopically distinct. The $T_1T_2$ conformer is unique and alone has $C_s$ symmetry.) For 2-propyl peroxy radical, the spectra of both conformers have been tentatively assigned.[18] For 1-propyl peroxy, the spectra of three of the five conformers have been tentatively assigned.[7]

For *n*-butyl peroxy, one must add a third dihedral angle between the $C_1-C_2-C_3$ and $C_2-C_3-C_4$ planes giving conformers labeled by $T_1(G_1^{(\prime)})T_2(G_2^{(\prime)})T_3(G_3^{(\prime)})$. Because for each set of dihedral angles there are three possible orientations (0, ±120°) there are $3^3 = 27$ possible conformations. There is a unique one, $T_1T_2T_3$, with $C_s$ symmetry. The remaining 26 have only $C_1$ symmetry and exist in mirror image pairs, giving another 13 spectroscopically distinct conformers for a total of 14. This results in the following unique conformers (all with mirror images except the first): $T_1T_2T_3$, $T_1T_2G_3$, $T_1G_2T_3$, $T_1G_2G_3$, $G_1T_2T_3$, $G_1T_2G_3$, $G_1T_2G_3'$, $G_1G_2T_3$, $G_1G_2'T_3$, $T_1G_2G_3$, $T_1G_2G_3'$, $G_1G_2G_3$, $G_1G_2G_3'$, and $G_1'G_2G_3$.

The appearance of the conformers of *sec*-butyl peroxy can be readily derived from those of 2-propyl peroxy by substituting one of the methyl H's by another methyl group. In the G conformer of 2-$C_3H_7O$ each of the six methyl H's are distinct, giving six *sec*-butyl peroxy conformers (each with G′ mirror images). There can be designated $G_1T_\alpha$, $G_1G_\alpha$, $G_1G_\alpha'$, $G_1T_\beta$, $G_1G_\beta$, and $G_1G_\beta'$, where $T_1(G_1^{(\prime)})$ denotes the orientation of the H−$C_2$−O and $C_2$−O−O dihedral angles. The $T_{\alpha/\beta}(G_{\alpha/\beta}')$ denotes whether the $C_1-C_2-C_3$ and $C_2-C_3-C_4$ dihedral angles are 0° or ±120°. The subscript $\alpha/\beta$ denotes whether the O is pointed toward/away from the $C_4$ methyl. The T form of 2-$C_3H_7O$ also has six substitution sites, but the corresponding ones on each methyl group are equivalent, so only three spectroscopically distinct conformers exist, given a total of nine distinct conformers for *sec*-butyl peroxy. For the T forms, we drop the $\alpha/\beta$ label ($T_1G_2$, $T_1T_2$,$T_1G_2'$) in favor of two to denote the $C_1-C_2-C_3$ and $C_2-C_3-C_4$ planes' orientations.

The conformers of isobutyl peroxy can be derived from the T and G forms of ethyl peroxy by substituting two methyl groups for the H's of the methyl group. For G ethyl peroxy there are three distinct substitutions yielding ($G_1T_2$, $G_1G_2$, $G_1G_2'$) and for T there are two distinct substitutions ($T_1T_2$, $T_1G_2$), giving a total of five conformers. In the conformer's designations $T_1(G_1)$ denotes the O−O−$C_1$ and the O−$C_1$−$C_2$ dihedral angle orientation whereas $T_2(G_1^{(\prime)})$ labels that of the O−$C_1$−$C_2$ and $C_2-C_3-C_4$ dihedral angles.

Finally, we can consider *tert*-butyl peroxy. Initially, one might assume that like methyl peroxy, it would have only one conformer, the analogue of the cis or staggered conformation (with $C_s$ symmetry). However, it is not at all clear that the trans or eclipsed conformer (also $C_s$ symmetry) analogue remains a saddle point. It might well also correspond to a minimum with the barrier to $O_2$ group rotation being in the $C_1$ conformation when the O and methyl H are truly eclipsed.

Finally, we should note that on the basis of the calculations[7,18] for the propyl peroxy conformers, we would expect all the butyl peroxy energies to be within 1−2 *kT* and so all have significant population at room-temperature equilibrium.

### 4. Observed Spectra and Assignments

To sort out the spectra of the various isomers and conformers of butyl peroxy, it is important to generate the radicals using both production methods. In the following we describe and correlate the results of the various approaches.

**4.1. Straight-Chain Butyl Peroxy Radicals.** Figure 2 shows the CRDS spectrum (middle trace) for the *n*-butyl peroxy radical produced following the direct photolysis of *n*-butyl bromide. There are clearly three distinct bands in the origin region closely enough spaced so that they are unlikely to constitute transitions to the $\tilde{A}$ state's excited vibrational levels. Rather they more likely constitute one "true" origin and two "hot bands" involving no change in vibrational excitation, e.g., either hot vibrational sequence bands or hot origin bands from low-lying thermally populated conformations. Probably a reasonable limit for the excitation energy of the originating level in either case is $<3kT \approx 600$ cm$^{-1}$; otherwise, the level would not be significantly populated. Normally, vibrational frequencies do not vary by more than ≈5−10% between the $\tilde{A}$ and $\tilde{X}$ states. Hence one would expect vibrational sequence bands to lie $\lesssim$50 cm$^{-1}$ of the origin. Applying this criterion to the *n*-butyl peroxy bands indicates that they likely arise from three (or more unresolved combinations) of the 14 possible conformers. One also notes corresponding sets of multiple bands roughly 500 and 900 cm$^{-1}$ higher in frequency. These likely arise from excitation of the CCO bend and O−O stretch, respectively. Because these are two of the three vibrations involving directly the $O_2$ chromophore we expect the greatest change in their equilibrium coordinates between the $\tilde{A}$ and $\tilde{X}$ states and correspondingly the most intensity in their fundamental excitation due to favorable Franck−Condon factors.

We have summarized the frequencies of the above transitions in Table 1 labeling the conformers A, B, and C in order of increasing origin frequency. Table 2 shows the frequencies of

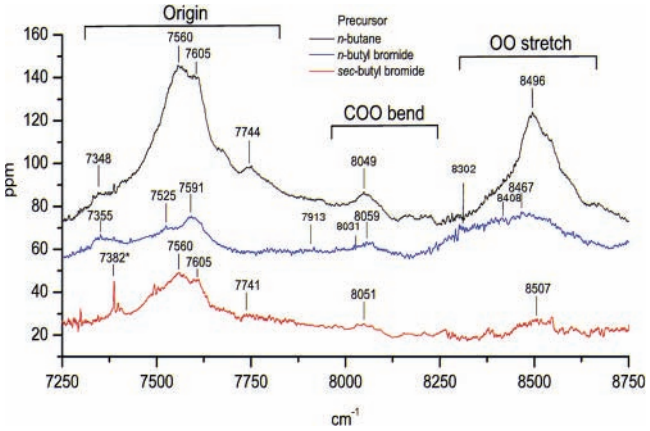


**Figure 2.** CRDS spectra of *n*-butyl and *sec*-butyl peroxy radicals. The top trace in black is the CRDS spectra of *n*-butyl and *sec*-butyl peroxy radicals produced by the hydrogen abstraction method, offset by 30 ppm for visualization purposes. The middle trace in blue is the CRDS spectrum of *n*-butyl peroxy radical produced by the direct photolysis method, offset by 60 ppm. The bottom trace in red is the CRDS spectrum of the *sec*-butyl peroxy radical produced by the direct photolysis method, with no offset. The peak labeled with an asterisk belongs to methyl peroxy radical. Approximate frequencies in $cm^{-1}$ are indicated for the major peaks. The *y*-axis denotes cavity loss in parts per million per pass and the *x*-axis is in wavenumbers. The same conventions hold for all the spectral plots. All the peaks listed in Table 1 are identified in the above traces. A few of the weakest lines are barely visible in the above traces but have been verified in independent observations.

**TABLE 1: Observed CRDS Band Frequencies[a] for the Various Butyl Peroxy Isomers[b]**

| peroxy isomer | conformers expected | conformers observed | | observed bands origin | C−O−O bend | O−O stretch |
|---|---|---|---|---|---|---|
| *n*-butyl | 14 | 3 | A | 7355 | 7913 | 8302 |
| | | | B | 7525 | 8031 | 8408 |
| | | | C | 7591 | 8059 | 8467 |
| *sec*-butyl | 9 | 2 | A | 7560 | 8051 | 8507 |
| | | | B | 7605 | | |
| isobutyl | 5 | 3 | A | 7306 | 7905 | 8242 |
| | | | B | 7480 | 7990 | 8462 |
| | | | C | 7536 | | 8537 |
| *t*-butyl | 1(2?) | 1 or 2 | A | 7757 | 8242 | 8695 |
| | | | B′ | 7895 | 8358 | |
| | | | C′ | 7994 | 8476 | |
| | | | D′ | 8094 | 8523 | |

[a] Frequencies are generally taken from the spectra produced by butyl bromide photolysis because less band overlap occurs in these spectra. In some cases the relative strength and/or isolation of a band in the spectrum produced by Cl atom abstraction dictated that the frequencies from that spectrum were the most reliable. In no case was there any discrepancy between different spectra greater than the experimental error ($\pm\approx 15$ $cm^{-1}$) in determining the band center. [b] Sets of bands likely belonging to a given conformer are labeled A, B, ...; the attribution of the primed labels for *tert*-butyl is presently unclear.

each conformer relative to the putative origin of conformer A and compares the shifts between the conformer origins to those of the *n*-propyl peroxy radicals. For the primary peroxy radicals, *n*-butyl and *n*-propyl, the resemblance is truly striking. In each case, conformer B is shifted $\approx 175$ $cm^{-1}$ to the blue and conformer C $\approx 235$ $cm^{-1}$ to the blue. Indeed, within experimental error, the conformer shifts are indistinguishable. Similarly, the absolute origin frequencies of conformer A for *n*-butyl and *n*-propyl peroxy are within 25 $cm^{-1}$.

This may seem a remarkable coincidence until one remembers that the conformers of *n*-butyl peroxy differ from *n*-propyl peroxy only by the addition of another methyl group to give a third dihedral angle defined by the orientation of the $C_1-C_2-C_3$ and $C_2-C_3-C_4$ planes. Given that this orientation of the hydrocarbon "tail" is far removed from the $O_2$ chromophore, it is unlikely to have a great effect on the observed spectrum.

**TABLE 2: Measured Shifts ($cm^{-1}$) in Frequency from the Origin Band of Conformer A, Whose Absolute Frequency Is Given in Parenthesis**

| primary conformer | *n*-butyl (7355) | isobutyl (7306) | *n*-propyl (7332) |
|---|---|---|---|
| A | 0 | 0 | 0 |
| B | 170 | 174 | 176 |
| C | 236 | 230 | 237 |

| secondary conformer | sec-butyl (7560) | isopropyl (7462) |
|---|---|---|
| A | 0 | 0 |
| B | 45 | 105 |

| tertiary conformer | *tert*-butyl (7757) |
|---|---|
| A | 0 |

Using the assignment[7] (see Table 2) of *n*-propyl peroxy as a guide, we can speculate on likely structural assignments for conformer A. Given that in propyl peroxy, conformer A is assigned to an unresolved combination of $T_1$ conformers, i.e., $T_1T_2$ and $T_1G_2$, we expect that conformer A in *n*-butyl peroxy likely corresponds to the same two orientations of the first two dihedral angles plus all possible distinct combinations of the third, i.e., the structures, $T_1T_2T_3$, $T_1T_2G_3$, $T_1G_2G_3$, $T_1G_2G_3'$, and $T_1G_2G_3'$.

In *n*-propyl peroxy, conformers B and C corresponded to $G_1$ conformers with a tentative assignment of conformer B to $G_1G_2$ and conformer C to the unresolved pair, $G_1T_2$ and $G_1G_2'$. We expect a similar pattern extends to *n*-butyl peroxy. If the above assignment to *n*-propyl peroxy is correct, then it is straightforward to extend it to *n*-butyl peroxy to assign the B bands to an unresolved combination of $G_1G_2T_1$, $G_1G_2G_3$, $G_1G_2'T_3$, and $G_1G_2G_3'$. This implies that the C band is attributable to the $G_1T_2G_3$, $G_1T_2G_3'$, $G_1T_2T_3$, $G_1G_2'G_3$, and $G_1G_2'G_3'$ conformers.

Figure 2 shows the CRDS spectrum (bottom trace) for *sec*-butyl peroxy radical from the direct photolysis of *sec*-butyl bromide. The band centered around 7560 $cm^{-1}$ likely represents the "true" origin of conformer A. The smaller band located near 8507 $cm^{-1}$ would be the corresponding O−O stretch transition for the *sec*-butyl peroxy radical. A small COO bend transition peak can be located near 8051 $cm^{-1}$. Returning to the origin region, the peak at 7605 $cm^{-1}$ is reproducible (see below for the discussion of the spectrum using H atom abstraction) and is likely to be a second conformer (conformer B). Although the third peak at 7741 $cm^{-1}$ could be another conformer or even possibly a vibrational hot band, we think a more likely explanation is that it is a transition to two quanta of the low-frequency hindered rotation (torsional) motion of the terminal O, with respect to the $O-C_1-C_2$ backbone which is predicted to have a fundamental of $\approx 100$ $cm^{-1}$ in the *n*-propyl peroxy radicals. The 1-quantum transition is forbidden[18] in the $C_s$ moelcules and may well remain weak in the $C_1$ molecules. The sharp structure that appears at 7382 $cm^{-1}$ can be attributed to the methyl peroxy radical.[19] Transitions arising from methyl peroxy radical were observed to some degree using both methods of peroxy radical production and with all six of the precursors as well as in prior experiments for the propyl peroxy radicals.[6]

Figure 2 shows the CRDS spectrum (top trace) that was recorded using the hydrogen abstraction method of butyl peroxy radical production. The precursor was *n*-butane, and both straight-chain peroxy isomers were produced. The large peak

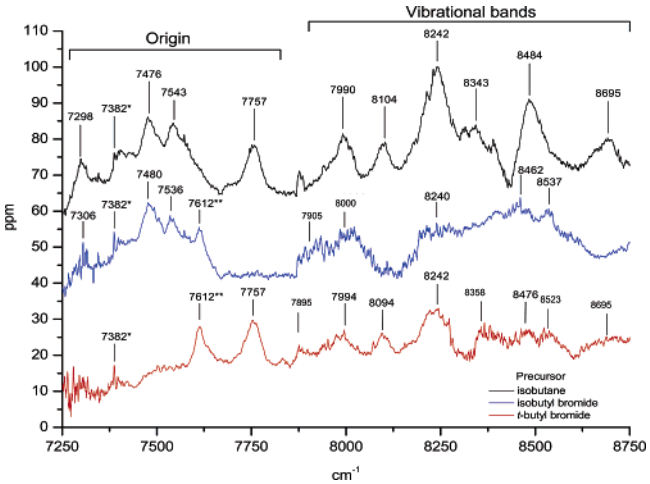


**Figure 3.** CRDS spectra of isobutyl and *tert*-butyl peroxy radicals. The top trace in black is the CRDS spectra of isobutyl and *tert*-butyl peroxy radicals produced by the hydrogen abstraction method, offset by 40 ppm for visualization purposes. The middle trace in blue is the CRDS spectrum of isobutyl peroxy radical produced by the direct photolysis method, offset by 25 ppm. The bottom trace in red is the CRDS spectrum of *tert*-butyl peroxy radical produced by the direct photolysis method, with no offset. The peaks labeled with one asterisk belong to the methyl peroxy radical. The peak labeled with two asterisks is long-lived a byproduct of the direct photolysis method. Approximate frequencies in $cm^{-1}$ are indicated for the major peaks.

centered around 7560 $cm^{-1}$ contains the origin of both *n*-butyl and *sec*-butyl peroxy radicals. The origin transition of another conformer of *n*-butyl peroxy radical observed in the direct photolysis method at 7355 $cm^{-1}$ has a slight peak at ≈7348 $cm^{-1}$. The origin of conformer B of *sec*-butyl peroxy radical is confirmed with the observation of the band at ≈7605 $cm^{-1}$. The oxygen−oxygen stretch for the most intense transition is observed at 8496 $cm^{-1}$. The peak at 8049 $cm^{-1}$ (8059 $cm^{-1}$ with direct photolysis) contains the COO bend. A summary of the transition frequencies observed for the straight-chain butyl peroxy radicals using both methods of production is shown in Table 1. In Table 2 we compare the 2-propyl and 2-butyl peroxy spectra. The similarity is not as striking as for *n*-propyl and *n*-butyl peroxy nor should we probably expect it to be given the difference in symmetry etc. However, the similarity is strong enough that a reasonable assignment of conformer B is to an unresolved combination of the conformers with the $G_1$ orientation of the H−$C_2$−O, and $C_2$−O−O planes. Correspondingly, the band in the spectrum attributed to conformer A is likely the corresponding unresolved combination of the conformers with the $T_1$ structure.

**4.2. Branched Butyl Peroxy Radicals.** Figure 3 shows the CRDS spectrum (middle trace) for isobutyl peroxy radical using the direct photolysis of isobutyl bromide. At least two conformers exist in the spectrum with origin frequencies around 7480 and 7536 $cm^{-1}$ referred to as conformers B and C, respectively. Though not particularly clear in the spectrum produced by direct photolysis, a third peak (at 7306 $cm^{-1}$ and denoted as conformer A) is clearly evident in the H abstraction spectrum (7298 $cm^{-1}$ in top trace and see discussion below) and cannot reasonably be assigned to *tert*-butyl peroxy. The peak near 7612 $cm^{-1}$ does not belong to the isobutyl peroxy radical but is rather a long-lived reaction product. The broad band centered around 8462 $cm^{-1}$ represents the oxygen−oxygen stretch transition for the observed conformers of isobutyl peroxy radical. The less intense band near 8000 $cm^{-1}$ arises from the COO bend.

Figure 3 shows the CRDS spectrum (bottom trace) for *tert*-butyl peroxy radical using the direct photolysis method. A clear origin band (conformer A) resides at 7757 $cm^{-1}$. The present value is of higher accuracy but is in good agreement with previous work (7800 $cm^{-1}$) on the *tert*-butyl peroxy radical, which employed photoelectron spectroscopy.[20] Also observed in the isobutyl peroxy radical spectrum, the long-lived product peak near 7612 $cm^{-1}$ does not belong to *tert*-butyl peroxy radical. Several bands exist further to the blue of the origin and their assignment is not obvious beyond the bands assigned in Table 2 to the C−C−O bend and to the O−O stretch of conformer A. The remaining bands do seem to appear as two triplets separated by the appropriate C−C−O bend frequency. These triplets are denoted B′, C′, and D′ in Table 1.

Figure 3 shows the CRDS spectrum that was recorded using the hydrogen abstraction method of production. The precursor was isobutane, and both branched isomers were produced. A summary of all the transition frequencies observed for the branched butyl peroxy radicals using both methods of production is shown in Table 1.

It now remains to suggest plausible assignments for the conformer bands of isobutyl (2-methyl-propyl) peroxy radical. Even though isobutyl peroxy is derived from a branched hydrocarbon precursor, it is important to remember that it is a primary radical and probably best compared to *n*-butyl peroxy, as is done in Table 2. As this table shows, the absolute frequency of the transition of conformer A of *n*-propyl and isobutyl peroxy radicals are within 30 $cm^{-1}$, and the shifts of conformers B and C are within 10 $cm^{-1}$. Ergo it is likely that the A conformer corresponds to the $T_1$ orientation of the O−O−$C_1$, and O−$C_1$−$C_2$ planes with any further changes in orientation down the hydrocarbon chain undetectable in the spectrum. Conformers B and C then correspond to a $G_1$ orientation. However, the unresolved contribution of different conformer structures to the B and C spectral peaks is not clear.

For *tert*-butyl peroxy, in analogy to methyl peroxy we initially expect and see one spectrum attributable to a single conformer. However, as was discussed in section 3, it is possible a second conformer exists for *tert*-butyl peroxy. Perhaps the set of peaks denoted B′, C′, and D′ are attrubutable to this conformer. If so, the explanation of the triplet is even more speculative. The only possibility that comes to mind is a series of sequence bands from a slightly hindered $O_2$ rotational motion in a very shallow potential minimum. This spectrum clearly deserves further investigation.

## 5. Reaction Chemistry and Kinetics

The availability of isomer, and even in some cases conformer, specific spectral line assignments opens the possibility of using the CRDS spectra to study reaction mechanisms and kinetics. Our apparatus is optimized for spectroscopic not kinetic studies. Nonetheless, considerable kinetic information can be obtained relatively simply, while always remembering its quantitative limitations.

We have been able to study two kinds of reactions involving the butyl peroxy radicals. In the first case, we consider the formation of the radicals. In particular, the resolved butyl radical isomer spectra offer useful insights into the kinetics of Cl atom attack on the chemically distinct H atoms of the alkane precursor. A second kind of kinetic study involves the destruction of the butyl peroxy radicals, which is generally via a self-reaction mechanism.[21] Simple kinetic experiments using CRDS spectral lines as a diagnostic enable us to follow the isomer, and possibly conformer, dependent kinetics.

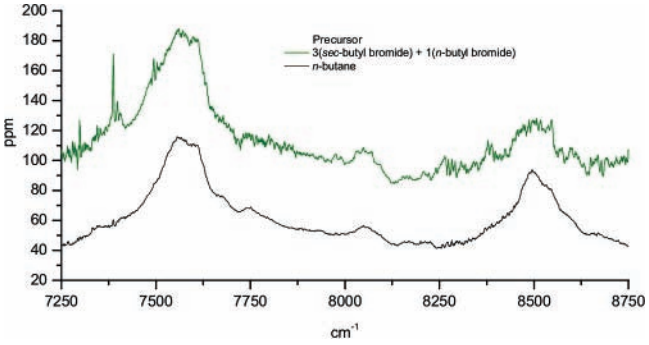


**Figure 4.** Comparison of CRDS spectra of the straight-chain butyl peroxy radicals. The top, green trace is the sum (offset by 50 ppm for visualization purposes) of the *n*-butyl peroxy radical spectrum and three times the *sec*-butyl peroxy radical spectrum using the direct photolysis method. The bottom, black trace (no offset) is the experimental CRDS spectrum using the hydrogen abstraction of *n*-butane method.

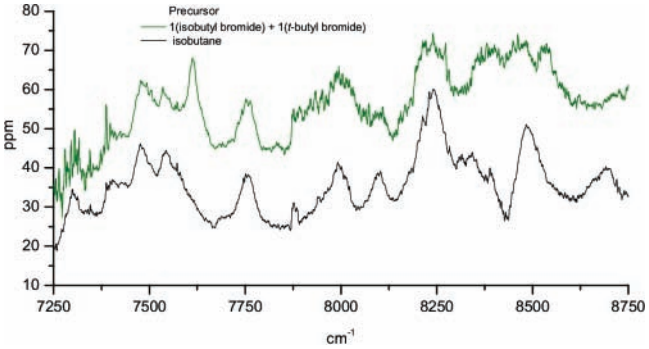


**Figure 5.** Comparison of CRDS spectra of the branched butyl peroxy radicals. The top, green trace is the sum of the isobutyl peroxy radical spectrum and the *tert*-butyl peroxy radical spectrum using the direct photolysis method, offset by 10 ppm for visualization purposes. The bottom, black trace is the experimental CRDS spectrum using the hydrogen abstraction of isobutane method, with no offset.

**5.1. Cl Atom Attack on Butane.** In the Cl atom based production of butyl peroxy radicals, the first step is H abstraction from butane, i.e.,

$$\mathrm{Cl} + n\text{-}\mathrm{C_4H_{10}} \begin{cases} \xrightarrow{k_p^n} \mathrm{HCl} + \mathrm{CH_3{-}(CH_2)_2{-}CH_2\bullet} \\ \xrightarrow{k_s^n} \mathrm{HCl} + \mathrm{CH_3 - \underset{\bullet}{CH}{-}CH_2{-}CH_3} \end{cases} \quad (4)$$

and

$$\mathrm{Cl} + iso\text{-}\mathrm{C_4H_{10}} \begin{cases} \xrightarrow{k_p^i} \mathrm{HCl} + \mathrm{(CH_3)_2CH{-}\overset{\bullet}{C}H_2} \\ \xrightarrow{k_t^i} \mathrm{HCl} + \overset{\bullet}{\mathrm{C}}{-}\mathrm{(CH_3)_3} \end{cases} \quad (5)$$

Under our experimental conditions, it is reasonable to assume that all of the butyl radical isomers produced by eqs 4 and 5 are quantitatively converted to the corresponding peroxy isomer.[22−24] To a first approximation, it is also reasonable to assume that the oscillator strength of the $\tilde{A}-\tilde{X}$ transition is isomer independent. In this case the intensity of the respective CRDS peroxy radical spectra is a good measure of the ratios $(k_p^n/k_s^n)$ and $(k_p^i/k_t^i)$.

In Figures 4 and 5, we show (bottom black traces) the CRDS spectra with *n*-butane and isobutane, respectively, as precursors. For Figure 4, the green trace (top) is a weighted sum of the CRDS spectra of the *n*-butyl and *sec*-butyl peroxy spectra, as obtained from the direct photolysis of the corresponding butyl bromide isomer. For Figure 5, the green trace (top) is a corresponding sum of the isobutane and *tert*-butyl peroxy isomers. In each the weighting factor has been adjusted to best match the experimental black trace. The derived weighting factors and corresponding values of the rate constant ratios are $(k_p^n/k_s^n) = 3.0(3)$ and $(k_p^i/k_t^i) = 1.0(2)$. The values are generally consistent with the results[25−28] from other measurements of these rate constant ratios by quite different means. For example, both refs 27 and 28 find the relative production of 1- and 2-butyl radicals to be 29(2)% and 74(4)%, respectively, whereas our results imply 25(10)% and 75(10)%. Reference 27 finds the 1- and *tert*-butyl production to be 65(4)% and 35(3)%, and our results yield approximately 50(10)% and 50(10)%. Given the available H's in *n*-butane, our experimental results imply that a secondary H's is ≈4.5 more labile than a primary H. For isobutane, the corresponding ratio for tertiary to primary H's is ≈9.0. Put slightly differently the relative reactivity to Cl atoms of p:s:t H atoms in butane is approximately 2:9:18.

**5.2. Butyl Peroxy Radical Self-Reaction.** Under our experimental conditions, the dominant chemical mechanism for removal of butyl peroxy radicals is expected to be self-reaction.[29] Although there is some uncertainty concerning the products of this reaction, the peroxy radical rate of decay should be describable by

$$\frac{\mathrm{d}[\mathrm{C_4H_9O_2}]}{\mathrm{d}t} = -k[\mathrm{C_4H_9O_2}]^2 \quad (6)$$

Integrating eq 4 yields

$$\frac{[\mathrm{C_4H_9O_2}]_0}{[\mathrm{C_4H_9O_2}]} = [\mathrm{C_4H_9O_2}]_0 kt + 1 \quad (7)$$

It is reasonable to equate $S_0/S$ to $[\mathrm{C_4H_9O_2}]_0/[\mathrm{C_4H_9O_2}]$ in eq 7 where $S_0$ is the baseline-subtracted CRDS signal of the butyl peroxy origin peak at the minimum time delay (50 $\mu$s), and $S$ is the baseline-subtracted signal at increasing delay times. Delay times are determined by the firing of the excimer laser photolyzing a specific butyl bromide isomer and the YAG pumped dye laser producing radiation for the CRDS experiment. Under our experimental conditions, time delays on the order of milliseconds are used to follow the kinetics.

A linear fit of $S_0/S$ versus time gives a slope that is equivalent to $k[\mathrm{C_4H_9O_2}]_0$. Figure 6 shows the decay of the origin band of *n*-butyl peroxy and the insert displays a linear fit of $S_0/S$ versus time with a slope determined to be 238 $s^{-1}$. The inverse of this slope yields a half-life of 4.2 ms. As noted earlier the initial concentration of *n*-butyl peroxy radicals is estimated to $\approx 6 \times 10^{14}$ $cm^{-3}$, based upon the butyl bromide photolysis cross-section. The self-reaction rate, $k_n$, for *n*-butyl peroxy radical is therefore estimated to be

$$k_n = \frac{1}{(0.0042\ \mathrm{s})(6 \times 10^{14}\ \mathrm{cm^{-3}})} = 4 \times 10^{-13}\ \mathrm{cm^3/(molecule{\cdot}s)} \quad (8)$$

Similar second-order rate plots were obtained monitoring the decay of *sec*-butyl and isobutyl peroxy radicals. We believe that the pressure of $N_2/O_2$ in the cell is sufficiently high so that these rates correspond to thermalized rate constants. For the *tert*-butyl peroxy radical, only a very slight time dependence (likely due to *tert*-butyl radical diffusion) was observed and only an upper limit to the rate constant could be determined.

The results for all butyl peroxy isomers are summarized in Table 3. Spectral lines corresponding to different conformers of a given isomer were also monitored. In all cases the decay

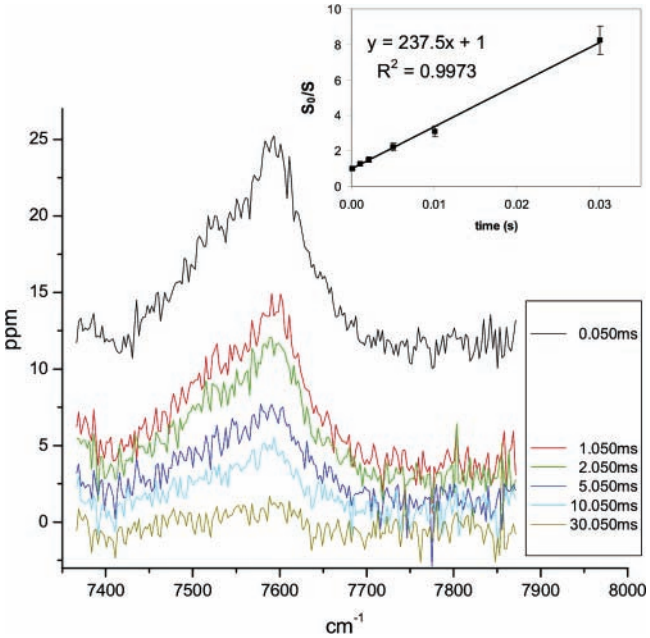


**Figure 6.** Intensity decrease of the origin band (conformer C) of the *n*-butyl peroxy radical using the direct photolysis method as the time delay between excimer and YAG is increased from 50 $\mu$s to 30 ms. The inset shows the relative signal intensity as a function of time with fit values for slope and linear regression coefficient.

**TABLE 3: Self-Reaction Rate Constants (cm$^3$/(molecule·s)) for Self-Reaction of Various Butyl Peroxy Isomers**

| | rate constant |
|---|---|
| *n*-butyl | $4 \times 10^{-13}$ |
| *sec*-butyl | $7 \times 10^{-14}$ |
| isobutyl | $1 \times 10^{-12}$ |
| *tert*-butyl | $<3 \times 10^{-14}$ |

rates of different conformers were the same within experimental error, which is not particularly surprising given the relatively slow kinetics of self-reaction compared to the likely rate of conformer conversion.

Due primarily to the large uncertainty in the estimate of $[C_4H_9O_2]_0$, the absolute values of the rate constants in Table 3 could be in error by up to a factor of 2−3. However, the relative rate constants should be much more reliable. The two primary peroxy radicals have the fastest decay rates, followed by *sec*-butyl, with *tert*-butyl peroxy radical slowest. Likely, this decrease in rate reflects steric hindrance to the O−O centers bonding, as an O four-membered ring is the suggested[29] transition state. Only for *tert*-butyl peroxy radical has a rate previously been reported[30] and it ($2 \times 10^{-17}$cm$^3$/(molecule·s)) is much less than our upper limit, and approximately $10^4$ less than our measured values for the other isomers.

## 6. Conclusions

The $\tilde{A}-\tilde{X}$ electronic spectra for the four isomers of butyl peroxy radical were reported for the first time using CRDS. Origin transitions as well as vibrational bands have been assigned for various conformers of *n*-butyl, *sec*-butyl, isobutyl, and *tert*-butyl peroxy isomers. The origin transition frequencies were in the region of 7250−7800 cm$^{-1}$, with vibrational bands around 7900−8250 cm$^{-1}$, which were mostly identified as COO bend transitions and oxygen−oxygen stretch transitions in the region of 8250−8700 cm$^{-1}$.

Two methods of peroxy radical production were used: direct photolysis of butyl bromide, and hydrogen abstraction from butane by Cl atoms following the photolysis of oxalyl chloride. The direct photolysis method allowed for an individual isomer to be produced but tended to have a lower signal/noise ratio. On the other hand, the hydrogen abstraction method produced two isomers simultaneously, yet was advantageous as an alternate method of butyl peroxy radical production resulting in greater signal/noise ratios.

A series of semiquantitative kinetic measurements were carried out using the assigned CRDS spectra to monitor the various butyl peroxy species. The relative reactivities of the p:s:t H atoms of butane to Cl atom attack were determined to be ≈2:9:18. The rate constants for butyl peroxy self-destruction were measured in an isomer specific manner again using the assigned CRDS spectra. Isomers vary in reaction rate by more than 100.

**Acknowledgment.** We acknowledge the financial support of this work by the Chemical Sciences, Geosciences and Biosciences Division, Office of Basic Energy Sciences, Office of Science, U.S. Department of Energy, via grant DE-FG02-01ER15172.

## References and Notes

(1) Curran, H. J.; Gaffuri, P.; Pitz, W. J.; Westbrook, C. K. *Combust. Flame* **1998**, *114*, 149.
(2) D'Anna, A.; Violi, A.; D'Alessio, A. *Combust. Flame* **2000**, *121*, 418.
(3) Wallington, T. J.; Nielsen, O. J. Peroxy Radicals and the Atmosphere. *Peroxy Radicals*; John Wiley and Sons: New York, 1997; pp 457−479 (see also references therein).
(4) Nielsen, O. J.; Wallington, T. J. Ultraviolet Absorption Spectra of Peroxt Radicals in the Gas Phase. *Peroxy Radicals*; John Wiley and Sons: New York, 1997); pp 72−73 (see also references therein).
(5) Pushkarsky, M. B.; J.Zalyubovsky, S.; Miller, T. A. *J. Chem. Phys.* **2000**, *112*, 10695.
(6) Zalyubovsky, S.; Glover, B.; Miller, T. A.; Hayes, C.; Merle, J. K.; Hadad, C. M. *J. Phys. Chem. A* **2005**, *109*, 1308.
(7) Tarczay, G.; Zalyubovsky, S.; Miller, T. A. *Chem. Phys. Lett.* **2005**, *406*, 81.
(8) Zalyubovsky, S. J.; Glover, B. G.; Miller, T. A. *J. Phys. Chem. A* **2003**, *107*, 7704.
(9) Scherer, J. J.; Paul, J. B.; O'Keefe, A.; Saykally, R. J. *Chem. Rev.* **1997**, *97*, 25−51.
(10) Nielsen, O. J.; Wallington, T. J. Methods of Preparing Organic Peroxy Radicals for Laboratory Studies. *Peroxy Radicals*; John Wiley and Sons: New York, 1997; pp 21−22 (see also references therein).
(11) Kozlov, S. N.; Orkin, V. L.; Huie, R. E.; Kurylo, M. J. *J. Phys. Chem. A* **2003**, *107*, 1333−1338.
(12) Ahmed, M.; Blunt, D.; Chen, D.; Suits, A. G. *J. Phys. Chem.* **1997**, *106*, 77617−7624.
(13) Baklanov, A. V.; Krasnoperov, L. V. *J. Phys. Chem. A* **2001**, *105*, 97−103.
(14) Jafri, J. A.; Phillips, D. H. *J. Am. Chem. Soc.* **1990**, *112*, 2586.
(15) Besler, B.; Sevilla, M.; MacNeille, P. *J. Phys. Chem.* **1986**, *90*, 6446.
(16) Rienstra-Kiracofe, J. C.; Allen, W. D.; Schaefer, H. F. S. *J. Phys. Chem. A* **2000**, *104*, 9823.
(17) Tarczay, G.; Miller, T. A. Unpublished results.
(18) Merle, J. K.; Hayes, C. J.; Zalyubovsky, S. J.; Miller, T. A.; Hadad, C. M. *J. Phys. Chem. A* **2005**, *109*, 3637.
(19) Pushkarsky, M. B.; Zalyubovsky, S. J.; Miller, T. A. *J. Chem. Phys.* **2000**, *112*, 10695−10700.
(20) Clifford, E. P.; Wenthold, P. G.; Garayev, R.; Lineberger, W. C.; DePuy, C. H.; Beirbaum, V. M.; Ellison, G. B. *J. Chem. Phys.* **1998**, *109*, 10293−10310.
(21) Ghigo, G.; Maranzana, A.; Tonachini, G. *J. Chem. Phys.* **2003**, *118*, 10575.
(22) Lenhardt, T. M.; McDade, C. E.; Bayes, K. D. *J. Chem. Phys.* **1980**, *72*, 304.
(23) Tsang, W. *J. Chem. Phys. Ref. Data* **1990**, *19*, 1−68.
(24) Dilger, H.; Stolmar, M.; Tregenna-Piggott, P. L. W.; Roduner, E. *Ber. Bunsen-Ges. Phys. Chem.* **1997**, *956*, 1101.
(25) Choi, N.; Pilling, M.; Seakins, P.; Wang, L. To be published.
(26) Seakins, P. W. *Abstracts of Papers, 228th ACS National Meeting, Philadelphia PA*; American Chemical Society: Washington, DC, 2004.
(27) Sarzynski, D.; Sztuba, B. *Int. J. Chem. Kinet.* **2002**, *34*, 651.
(28) Tyndall, G. S.; Orlando, J. J.; Wallington, T. J.; Dill, M.; Kaiser, E. W. *Int. J. Chem. Kinetics* **1997**, *29*, 43.
(29) Lesclaux, R. Combination of Peroxy Radicals in the Gas Phase. *Peroxyl Radicals*; John Wiley and Sons: New York, 1997; p 86.
(30) Wallington, T. J.; Dagaut, P.; Kurylo, M. J. *Chem. Rev.* **1992**, *92*, 667−710.